

Comparison of smoothed point interpolation methods in linear static problems

Samir S. Saliba¹, Lapo Gori¹, Roque L. S. Pitangueira¹

¹Structural Engineering Department, Federal University of Minas Gerais
Avenida Antônio Carlos, 6627, 31270-901, Belo Horizonte/MG, Brazil
samirsaliba@yahoo.com, lapo@dees.ufmg.br, roque@dees.ufmg.br

Abstract. Smoothed point interpolation methods (S-PIM), when compared with the standard finite element method (FEM) in the study of static linear problems, present interesting results due certain characteristics of their formulation. In general, meshfree methods have been shown to be more accurate and efficient. The proposed study aims to present a comparison between the Node-Based Smoothed Radial Point Interpolation Method with polynomial reproduction (NS-RPIMp), Edge-Based Smoothed Radial Point Interpolation Method with polynomial reproduction (ES-RPIMp) and Cell-Based Smoothed Radial Point Interpolation Method with polynomial reproduction (CS-RPIMp), applied to static linear-elastic problems. Several numerical simulations, performed using different strategies for support nodes selection based on the T-schemes (T3-, T4-, T6/3- and T2L-schemes), are presented, providing a relevant amount of results that allow to understand the behaviour of each one of these methods and schemes with respect to the accuracy and convergence rate.

Keywords: Smoothed point interpolation methods (S-PIMs), Node-based, Edge-base, Cell-based, Meshfree methods

1 Introduction

One of the main objectives of meshfree methods is to build a field function approximated totally in terms of nodes, in order to ease the discretization of a domain, which in many cases is laborious when it is necessary to construct a mesh for this purpose.

The starting point of meshfree, according to Belytschko et al. [1], was the smoothed particle hydrodynamics (SPH) method, presented by Gingold and Monaghan [2] and Lucy [3] in 1977. From this point on, many other methods were developed, among them the diffuse element method (DEM), introduced by Nayroles et al. [4], the element free Galerkin (EFG) method, proposed by Belytschko et al. [5], the reproducing kernel particle method (RKPM), developed by Liu and Chen [6], the meshless local Petrov-Galerkin (MLPG) method, introduced by Atluri and Zhu [7] and finally the point interpolation method (PIM), proposed by Liu and Gu [8].

Compared to methods based on approximation, such as the EFG, the PIM brought some advantages, such as the Kronecker delta function property, but some problems came together and to overcome these issues one of the proposals was the use of a weakened-weak (W^2) formulation combined with the G-space theory, which serve as the foundations for smoothed point interpolation methods (S-PIM).

This paper presents S-PIM models applied to linear static structural problems. The node-based smoothing point interpolation method (NS-PIM), edge-based smoothing point interpolation method (ES-PIM) and cell-based smoothing point interpolation method (CS-PIM) together with a T-scheme for selecting nodes support were applied in two simulations to present the performance of these methods when compared to the finite element method (FEM). The simulations were performed using the open-source software **INSANE**¹.

¹More informations on the project can be found at <https://www.insane.dees.ufmg.br/>; the development code is freely available at the Git repository <http://git.insane.dees.ufmg.br/insane/insane.git>.

2 Smoothed point interpolation methods (S-PIMs)

S-PIM models stand out due to the unique characteristics of their formulation based on the weakened-weak form. According to Liu and Zhang [9], these models were developed with the objective of being robust and easy to use. The use of triangular background cells in two-dimensional domains makes it easy to automate the discretization of complicated problems, the G-space theory corrects compatibility issues, ensures convergence and stability, low interpolation order allows them to be applied in a wide range of problems and the possibility of employing small numbers of nodes in the support domains makes them computationally efficient.

Unlike other meshfree methods, S-PIM models require the construction of smoothed strain fields, which are performed from a set of smoothing domains where the strain is assumed to be uniform. These smoothing domains are a tessellation of the problem domain into subdomains that must cover it without overlaps or gaps. The way these smoothing domains will be formed and the quantity, is related to the specific S-PIM model, and can be based on a node, edge or cell of the background mesh.

2.1 Radial point interpolation method with polynomials reproduction

The approximation of displacement field $u(\mathbf{x})$ at a point \mathbf{x} , in meshfree methods, is expressed as

$$u(\mathbf{x}) = \sum_{i=1}^n \phi_i(\mathbf{x})u_i, \quad (1)$$

where n is a set of nodes, ϕ_i is the nodal shape function for the i th node and u_i is the nodal displacement at the i th node.

Radial point interpolation method with polynomials reproduction (RPIMp), presented by Liu and Gu [8], combines radial basis functions (RBF) and polynomials basis in the shape function. Thus, the approximation of displacement field given by eq. (1) can be rewritten by

$$u(\mathbf{x}) = \sum_{i=1}^n R_i(\mathbf{x})b_i + \sum_{j=1}^m p_j(\mathbf{x})a_j = \mathbf{R}^T(\mathbf{x})\mathbf{b} + \mathbf{p}^T(\mathbf{x})\mathbf{a} = \begin{bmatrix} \mathbf{R}^T(\mathbf{x}) & \mathbf{p}^T(\mathbf{x}) \end{bmatrix} \begin{bmatrix} \mathbf{b} \\ \mathbf{a} \end{bmatrix}, \quad (2)$$

where n is a set of nodes in the neighborhood of \mathbf{x} , m is the number of polynomial base functions, b_i and a_j are coefficients associated to the RBFs and polynomials, respectively, R_i is the radial base function and p_j the monomials of the polynomial base.

The coefficients associated to the RBFs and polynomials functions, b_i and a_j , can be determined satisfying eq. (2) at the n nodes within the support domain. Therefore, eq. (2) can be rewritten in matrix form by

$$\begin{bmatrix} \mathbf{u} \\ \mathbf{0} \end{bmatrix} = \begin{bmatrix} \mathbf{R}_Q & \mathbf{P}_m \\ \mathbf{P}_m & \mathbf{0} \end{bmatrix} \begin{bmatrix} \mathbf{b} \\ \mathbf{a} \end{bmatrix} = \mathbf{G} \begin{bmatrix} \mathbf{b} \\ \mathbf{a} \end{bmatrix}, \quad (3)$$

where \mathbf{G} is the combined moment matrix composed by

$$\mathbf{R}_Q = \begin{bmatrix} R_1(r_1) & R_2(r_1) & \dots & R_n(r_1) \\ R_1(r_2) & R_2(r_2) & \dots & R_n(r_2) \\ \vdots & \vdots & \ddots & \vdots \\ R_1(r_n) & R_2(r_n) & \dots & R_n(r_n) \end{bmatrix}, \quad \mathbf{P}_m = \begin{bmatrix} P_1(\mathbf{x}_1) & P_2(\mathbf{x}_1) & \dots & P_m(\mathbf{x}_1) \\ P_1(\mathbf{x}_2) & P_2(\mathbf{x}_2) & \dots & P_m(\mathbf{x}_2) \\ \vdots & \vdots & \ddots & \vdots \\ P_1(\mathbf{x}_n) & P_2(\mathbf{x}_n) & \dots & P_m(\mathbf{x}_n) \end{bmatrix}. \quad (4)$$

Manipulating eq. (3) and replacing it in eq. (2), the approximation of displacement field can be rewritten as follows

$$u(\mathbf{x}) = \begin{bmatrix} \mathbf{R}^T(\mathbf{x}) & \mathbf{p}^T(\mathbf{x}) \end{bmatrix} \mathbf{G}^{-1} \begin{bmatrix} \mathbf{u} \\ \mathbf{0} \end{bmatrix}, \quad (5)$$

where the shape functions is given by

$$\phi(\mathbf{x}) = \begin{bmatrix} \mathbf{R}^T(\mathbf{x}) & \mathbf{p}^T(\mathbf{x}) \end{bmatrix} \mathbf{G}^{-1}. \quad (6)$$

RPIMp shape functions satisfy the Kronecker delta property, that is an important feature because it allows a straightforward imposition of boundary conditions.

2.2 T-schemes for nodes selection

The same background mesh used to build the smoothing domains can also be used to select the nodes in the support domain that will be used to build the shape functions.

Due to the ease of creation in addition to other important aspects, generally triangular type background meshes are used to discretize the domain, thus allowing the use of the so-called T-schemes.

According to Liu and Zhang [9, 10], T-schemes have been found to be most practical, robust, efficient and works well for the S-PIM models. Among the various existing schemes, the following are used in this work: T3-, T4-, T6/3- and T2L-scheme.

2.3 Construction of the Smoothing Domains

In the construction of the smoothing domains, two requirements are imposed: there must be no gaps or overlap between subdomains and they must completely cover the entire problem domain. The S-PIM models are derived from the way the smoothing domains are built, which can be: node-base, edge-base and cell-base.

For the node-based smoothing point interpolation method (NS-PIM) [11], the smoothing domains are built around each existing node in the domain. Taking a node as a reference, the centroids of the background cells are connected to the mid-edge-points that are incident to the node, as shown in Fig. 1a.

In the edge-based smoothing point interpolation method (ES-PIM) [12], the smoothing domains are created for each edge of the background cells. For this, the endpoints of the edges are connected to the centroid of the adjacent cells, Fig. 1b.

For cell-based smoothing point interpolation method (CS-PIM) [13, 14], each cell of the background mesh corresponds to a smoothing domain, as illustrated in Fig. 1c. This makes CS-PIM similar to the finite element method (FEM).

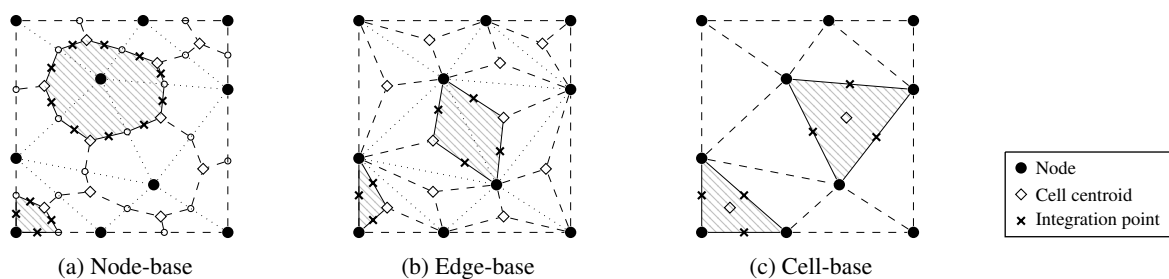


Figure 1. Smoothing domains

3 Numerical simulations

This section illustrates the results of the numerical simulation of two structural problems, and aims to point out the convergence properties of the three S-PIM models discussed in the previous sections, combined with different T-schemes for support nodes selection. The T4-scheme was used only in CS-RPIMp and T3-scheme in ES- and NS-RPIMp, the others schemes were used in the three S-PIMs models. For comparison purposes, the results obtained by the FEM were plotted together with the results obtained in each S-PIM model.

3.1 L-shaped panel

The L-shaped panel illustrated in Fig. 2 has a thickness equal to 100 mm and is subjected to a vertical force $F = 1400$ N. The material parameters experimentally obtained by Winkler et al. [15] and adopted in the numerical simulation are: Young's modulus $E = 25850$ MPa and Poisson's ratio $\nu = 0.18$.

The meshfree shape functions were constructed with the radial point interpolation method with polynomials reproduction, using the exponential radial function with $c = 0.002$ and 3 polynomials terms. The discretizations used in each S-PIM model are shown in Figs. 3 to 5.

The vertical displacement of the point of load application obtained in the analysis of the L-shaped panel is shown in Fig. 6.

The results obtained from the S-PIM models, the CS- and the ES-RPIMp followed in most cases the same

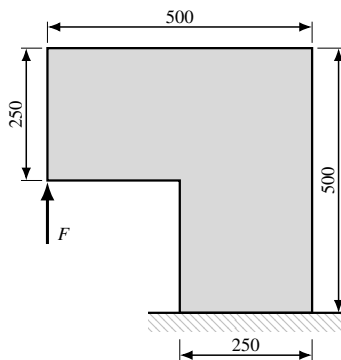


Figure 2. L-shaped panel (measures in *mm*)

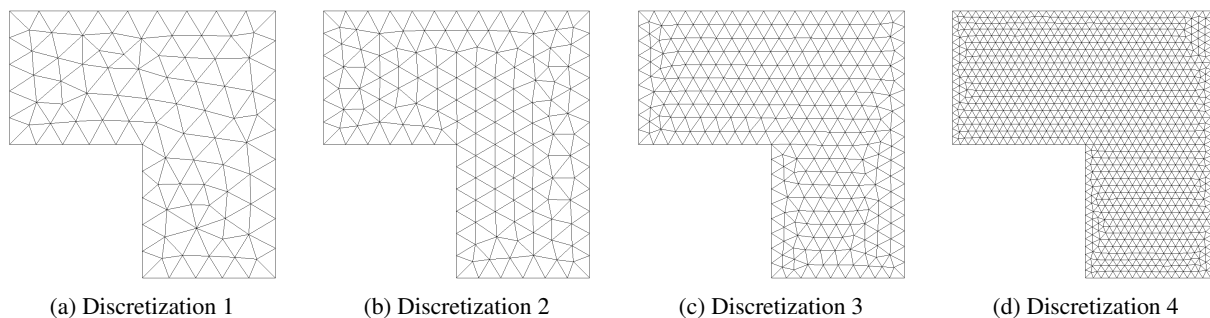


Figure 3. FEM and CS-RPIM discretizations

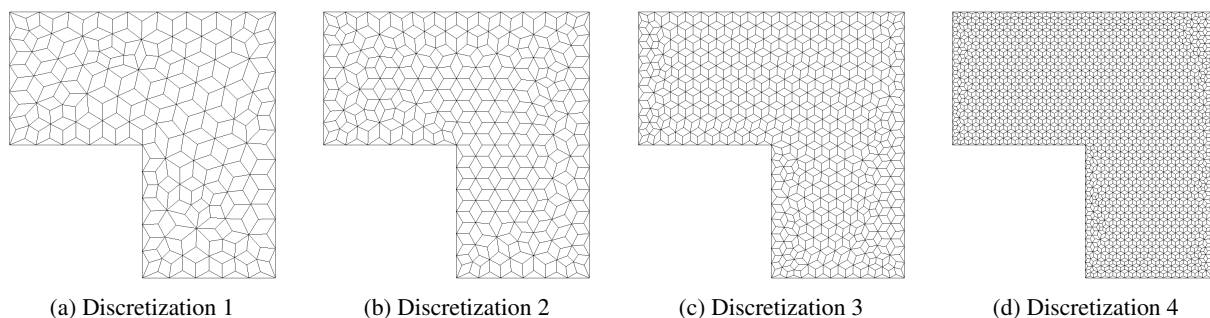


Figure 4. ES-RPIM discretizations

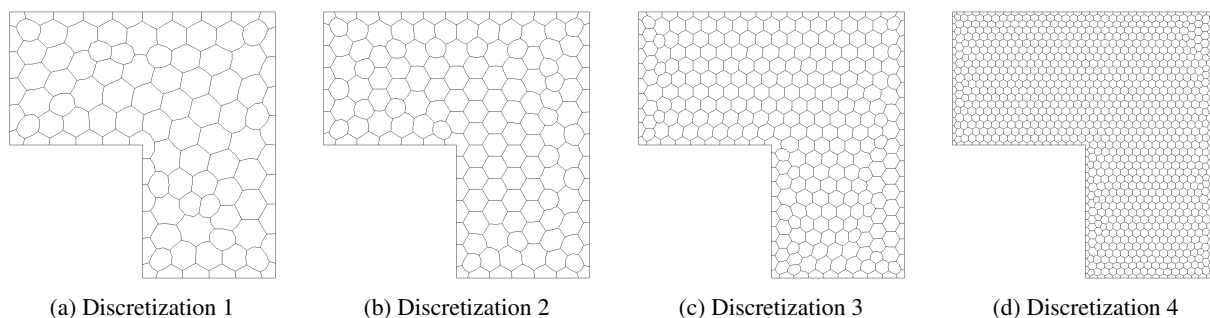


Figure 5. NS-RPIM discretizations

tendency presented by the FEM, the displacements increasing due to the refinement of the domain. On the other hand, as expected, NS-RPIM presented an opposite behaviour. The CS-RPIM when applied together the T6/3- and T2L-scheme showed convergence superior to the FEM, whereas the T4-scheme did not present a biased behaviour. The ES-RPIM showed a higher convergence than the FEM and also a biased behaviour for the three nodal selection schemes. NS-RPIM, as previously mentioned, has a tendency starting from higher values. In addition, only the T3-scheme that presented a tendency, the other two schemes suffered oscillations with refinement. In general, all schemes oscillated in at least one situation, however the results obtained with the schemes that select

a greater number of nodes, T6/3- and T2L-scheme, showed more promising.

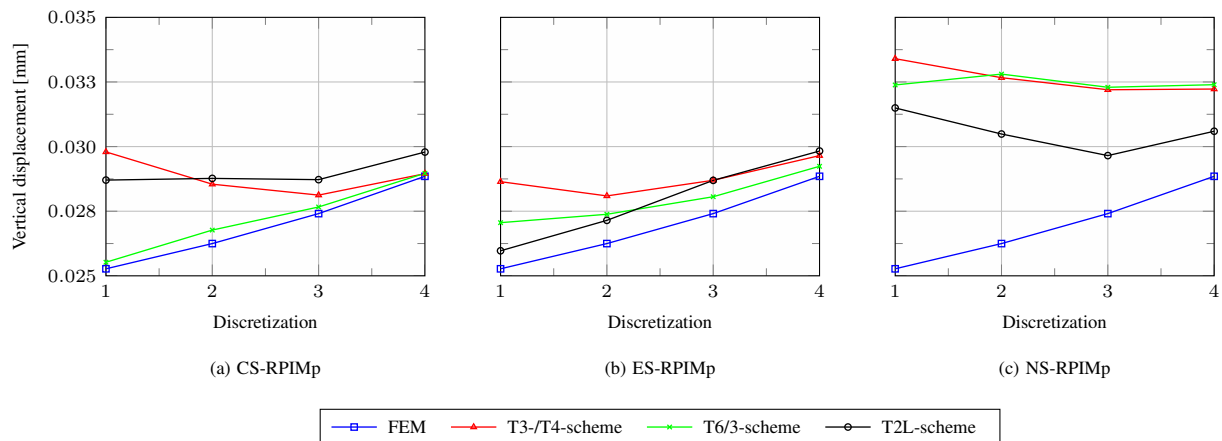


Figure 6. L-shaped panel - Convergence

3.2 Three-point bending test

The beam illustrated in Fig. 7 has a thickness equal to 50 mm and it is subjected to a vertical force $F = 200$ N. For the numerical simulation, the following material parameters experimentally obtained by Petersson [16] were used: Young's modulus $E = 30000$ MPa and Poisson's ratio $\nu = 0.2$.

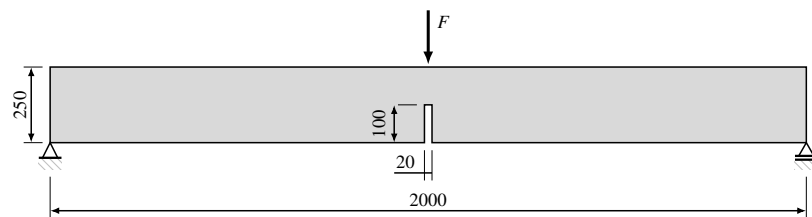


Figure 7. L-shaped panel (measures in mm)

The meshfree shape functions were constructed with the radial point interpolation method with polynomials reproduction, using the exponential radial function with $c = 0.002$ and 3 polynomials terms. The discretizations used in each S-PIM model are shown in Figs. 8 to 10.

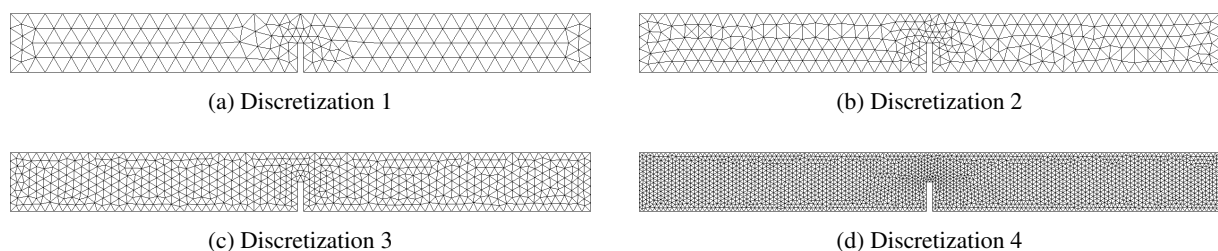


Figure 8. FEM and CS-RPIMp discretizations

The vertical displacements of the point of load application obtained in the analysis of the L-shaped panel are shown in Fig. 11.

In the three-point bending test, the CS-RPIMp and ES-RPIMp methods using the scheme that selects the smallest number of support nodes, in the case T4 and T3, respectively, showed results that hardly changed with the mesh. For these two methods, the other two schemes employed also showed a tendency of convergence superior to the FEM. The CS-RPIMp, when using the T3- and T2L-scheme, presented a small oscillation due to the refinement of the discretization, with the T6/3-scheme, the vertical displacement increased as the discretization increased. ES-RPIMp and NS-RPIMp, regardless of the scheme used, presented results without oscillations, showing a behaviour

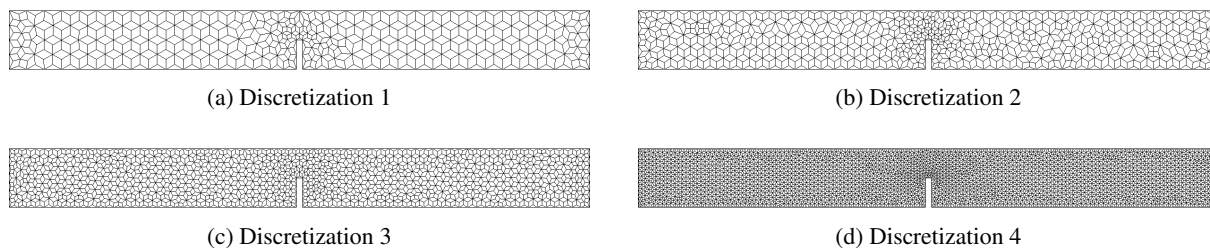


Figure 9. ES-RPIM discretizations

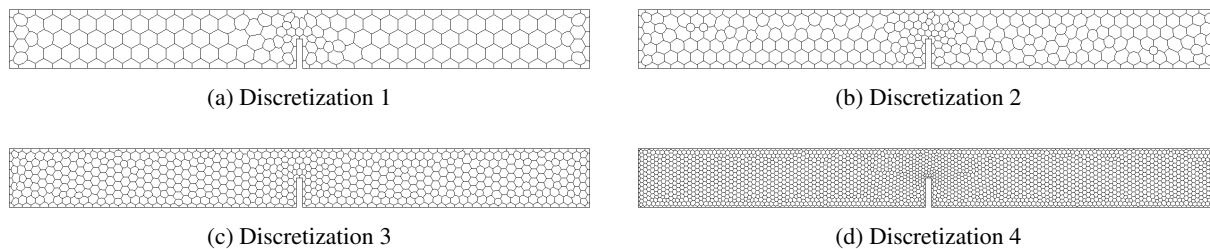


Figure 10. NS-RPIM discretizations

that tends to a value as the discretization refinement occurs. Among of the three methods employed, only the NS-RPIM approaches by higher vertical displacement values, taking the FEM results as reference. The T2L-scheme showed the best results for this method. The T6/3-scheme was the only one that did not present oscillations in the results for all methods in this simulation.

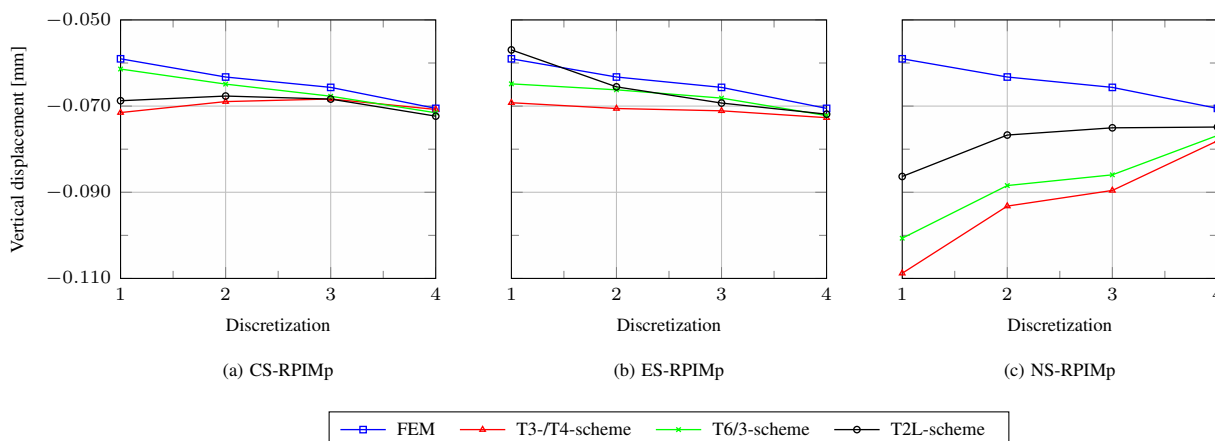


Figure 11. L-shaped panel - Convergence

4 Conclusions

An investigation to understand the behaviour of CS-, ES- and NS-RPIM methods when applied to linear static structural problems was presented. To perform, two numerical problems were analyzed from four different discretizations and different nodal selection strategies, in this case T3-, T4-, T6/3- and T2L-scheme. As can be seen, the results obtained in the simulations showed that the NS-RPIM is more flexible than the others S-PIM models and the FEM. The convergence rate and accuracy of the CS- and ES-RPIM methods is higher or in the same order as the FEM. In the most refined discretizations, the T3-, T4- and T6/3-scheme present very similar results in all situations. In general, when comparing the methods, the ES-RPIM proved to be more attractive than the other two meshfree methods, as it presented the results that less oscillate regardless of the scheme used in the simulations. Regarding strategy, it was observed that T6/3-scheme as well as ES-RPIM was the one that oscillated the least. In particular, the combination that presented the results with the best behaviour was the ES-RPIM with T6/3-scheme.

Acknowledgements. The authors gratefully acknowledge the support from the Brazilian research agencies CAPES (Coordenação de Aperfeiçoamento de Pessoal de Nível Superior), FAPEMIG (Fundação de Amparo à Pesquisa do Estado de Minas Gerais; grant PPM-00747-18), and CNPq (Conselho Nacional de Desenvolvimento Científico e Tecnológico; grant 309515/2017-3).

Authorship statement. The authors hereby confirm that they are the sole liable persons responsible for the authorship of this work, and that all material that has been herein included as part of the present paper is either the property (and authorship) of the authors, or has the permission of the owners to be included here.

References

- [1] Belytschko, T., Krongauz, Y., Organ, D., Fleming, M., & Krysl, P., 1996. Meshless methods: An overview and recent developments. *Computer Methods in Applied Mechanics and Engineering*, vol. 139, pp. 3–47.
- [2] Gingold, R. A. & Monaghan, J. J., 1977. Smoothed particle hydrodynamics: theory and application to non-spherical stars. *Mon. Not. Roy. Astron. Soc.*, vol. 181, pp. 375–389.
- [3] Lucy, B. L., 1977. A numerical approach to the testing of the fission hypothesis. *The Astronomical Journal*, vol. 82, n. 12, pp. 1013–1024.
- [4] Nayroles, B., Touzot, G., & Villon, P., 1992. Generalizing the finite element method: Diffuse approximation and diffuse elements. *Computational Mechanics*, vol. 10, pp. 307–318.
- [5] Belytschko, T., Lu, Y. Y., & Gu, L., 1994. Element-free galerkin methods. *International Journal for Numerical Methods in Engineering*, vol. 37, pp. 229–256.
- [6] Liu, W. K. & Chen, Y., 1995. Wavelet and multiple scale reproducing kernel methods. *International Journal for Numerical Methods in Fluids*, vol. 21, pp. 901–931.
- [7] Atluri, S. N. & Zhu, T., 1998. A new meshless local petrov-galerkin (MLPG) approach in computational mechanics. *Computational Mechanics*, vol. 22, pp. 117–127.
- [8] Liu, G. R. & Gu, Y. T., 2001. A local radial point interpolation method (LRPIM) for free vibration analyses of 2-D solids. *Journal of Sound and Vibration*, vol. 246(1), pp. 29–46.
- [9] Liu, G. R. & Zhang, G. Y., 2013. *Smoothed point interpolation methods: G space theory and weakened weak forms*. World Scientific Publishing Co. Pte. Ltd.
- [10] Liu, G. R., 2009. *Meshfree methods: Moving beyond the finite element method*. CRC Press, 2nd edition.
- [11] Wu, S. C., Liu, G. R., Zhang, H. O., & Zhang, G. Y., 2009. A node-based smoothed point interpolation method (NS-PIM) for thermoelastic problems with solution bounds. *International Journal of Heat and Mass Transfer*, vol. 52, pp. 1464–1471.
- [12] Wu, S. C., Liu, G., Cui, X. Y., Nguyen, T., & Zhang, G. Y., 2010. An edge-based smoothed point interpolation method (ES-PIM) for heat transfer analysis of rapid manufacturing system. *International Journal of Heat and Mass Transfer*, vol. 53, pp. 1938–1950.
- [13] Liu, G. R. & Zhang, G. Y., 2009. A normed G space and weakened weak (W^2) formulation of a cell-based smoothed point interpolation method. *International Journal of Computational Methods*, vol. 6(1), pp. 147–179.
- [14] Zhang, G. & Liu, G. R., 2010. A meshfree cell-based smoothed point interpolation method for solid mechanics problems. In *AIP Conference Proceedings*, volume 1233, pp. 887–92, Hong Kong- Macau(China). AIP.
- [15] Winkler, B., Hofstetter, G., & Lehar, H., 2004. Application of a constitutive model for concrete to the analysis of a precast segmental tunnel lining. *International Journal for Numerical and Analytical Methods in Geomechanics*, vol. 28, pp. 797–819.
- [16] Petersson, P.-E., 1981. Crack growth and development of fracture zones in plain concrete and similar materials. In *Tech. Rep. TVBM-1006, Division of Building Materials*, Lund (Sweden). Lund Institute of Technology.